Materials and Design 87 (2015) 82–94

Contents lists available at ScienceDirect

Materials and Design

journal homepage: www.elsevier.com/locate/jmad

Preparation, structure and properties of hybrid materials based on geopolymers and polysiloxanes

Giuseppina Roviello [a,*], Costantino Menna [b], Oreste Tarallo [c], Laura Ricciotti [a], Claudio Ferone [a], Francesco Colangelo [a], Domenico Asprone [b], Rosa di Maggio [d], Elisa Cappelletto [d], Andrea Prota [b], Raffaele Cioffi [a]

[a] Dipartimento di Ingegneria, Università di Napoli 'Parthenope', INSTM Research Group Napoli Parthenope, Centro Direzionale Napoli, Isola C4, 80143 Napoli, Italy
[b] Dipartimento di Strutture per l'Ingegneria e l'Architettura, Università degli Studi di Napoli "Federico II", Napoli 80125, Italy
[c] Dipartimento di Scienze Chimiche, Università degli Studi di Napoli "Federico II", Complesso Universitario di Monte S. Angelo, Via Cintia, 80126 Napoli, Italy
[d] Dipartimento di Ingegneria Civile, Ambientale e Meccanica, Università di Trento, Via Mesiano, 77, Trento 38123, Italy

ARTICLE INFO

Article history:
Received 23 April 2015
Received in revised form 31 July 2015
Accepted 1 August 2015
Available online 4 August 2015

Keywords:
Alkali activated cement
Hybrid
SEM
Spectroscopy
Mechanical properties

ABSTRACT

New hybrid materials with no phase separation up to nanometric level were obtained by performing the *in situ* co-reticulation of an aluminosilicate source (metakaolin), a mixture of dialkylsiloxane oligomers with different degrees of polymerization and an alkaline solution. As supported by SEM and NMR analyses, these hybrid materials are characterized by a highly interpenetrated structure due to the chemical similarity between the components, resulting in excellent physical and mechanical properties compared to neat geopolymers. These promising results represent a further step in developing alternative "low-carbon" binders (as also geopolymers) with improved engineering properties in the concrete technology. The enhanced mechanical properties, along with the high fire resistance, also suggest their utilization for structural applications as heat insulating and heat-resistant panels for the construction industry, and in the production of heat-resistant protective coatings or adhesives for technologically advanced uses.

1. Introduction

Hybrid materials are not simply physical mixtures of organic and inorganic components but they can be defined as nanocomposites, in which two components are intimately mixed and at least one of the domain of the components has a dimension ranging from a few angstroms to several nanometers [1]. In particular, organic–inorganic hybrids play a key role in the development of advanced functional materials since their chemical and physical properties are not only the sum of the single contributions of each phase, but they are unique in respect to those of the parent phases, deriving from the synergistic interaction between the phases that arises from interfacial forces at the nanometric scales [1].

During the last years the number of patents and articles related with nanostructured hybrid composite materials has increased, and among them, a particularly interesting area involves geopolymer based ones [2–4].

Geopolymers, also referred to as "alkali-activated cements" or "alkali-activated aluminosilicates" [5], show interesting excellent mechanical properties, low shrinkage, thermal stability, freeze–thaw, chemical and fire resistance, long term durability and recyclability. For these reasons, their application covers many fields.

First of all, geopolymer based materials are widely studied as a "low-carbon" binder alternative with respect to Ordinary Portland Cement (OPC) in new Sustainable Buildings due to several environmental advantages, such as a lower CO_2 footprint and low production temperature. In addition, geopolymer technology entails inexpensive and ecofriendly synthetic procedures involving raw materials such as clays [6,7] and other natural silico-aluminates [8] as well as industrial wastes like coal fly ash [5,9–12].

However, the brittle behavior and the unknown long-term durability of aluminosilicate geopolymers represent some of the limits for their extensive application as structural materials. In addition, the different rheological behaviors and the scarce compatibility with polymeric materials restrict the possible number of "*in-situ*" applications in construction activities. Up to now, in order to find a solution to those problems, the development of geopolymer-based composite materials has received great attention [13–15]. Different fillers can be introduced into the geopolymeric matrix, in order to improve its mechanical and physical properties. Among them, a great interest has been devoted, up to now, to polymeric fillers due to their low density, chemical stability and easy processing [16,17].

In these composites, the organic component is usually dispersed in the inorganic matrix by a simple mixing procedure, in which the polymer is added to geopolymeric slurry as powder, fibers, emulsion, sometimes in the presence of compatibilizing agents [18–22]. The obtained organic–geopolymer composites show improved mechanical strengths,

* Corresponding author.
E-mail address: giuseppina.roviello@uniparthenope.it (G. Roviello).

http://dx.doi.org/10.1016/j.matdes.2015.08.006
0264-1275/

but generally, the beneficial effect is limited to very low amount of polymer (about 1% by weight) since higher polymer concentration usually causes a tremendous decrease in the mechanical properties [22]. This is probably due to the limited compatibility between organic and inorganic phases, as well as to their poor chemical interaction. In order to overcome this problem, compatibilizing agents are usually added to the composite mixture, thus reducing segregation problems which can compromise the homogeneity and the final performances of the material.

Recently, we proposed an alternative approach to obtain a new class of hybrid composite materials based on geopolymers in which an organic epoxy resin content (up to 25 wt.%) was effectively incorporated within the geopolymer matrix without any additive [23–25]. This result was achieved by means of a careful choice of the chemical nature and structure of the organic phase, *i.e.* its composition was tailored in order to form the greatest number of hydroxyl tails during the epoxy ring opening reaction (Fig. 1), and by carrying out its polymerization directly *in situ* and simultaneously to the geopolymeric polycondensation reaction.

By following this procedure, a good compatibility up to micrometric level was achieved between the inorganic geopolymeric phase and the epoxy resins, allowing the obtainment of non-flammable composite materials showing improved toughness with respect to the neat geopolymer that could provide convenient, lightweight and durable solutions not only for structural applications [26,27] but, depending on the chemical nature of the resin, also a smart alternative to conventional metallic or ceramic composites.

In order to obtain a closer interaction between organic and inorganic components within a geopolymer-based material, in the present study we extend the synthetic approach described in [23] to silicone rubber precursors, trying to exploit the chemical similarity between polysiloxanes and polysialates. Polysiloxanes, in fact, are inorganic polymers based on a Si–O chain, containing alkyl or aryl groups bonded to Si atom (R, R′, Fig. 2), thus possessing a backbone very similar to that one characterizing geopolymers.

In particular, the synthetic approach developed by us [23–25] is used to obtain, for the first time, novel geopolymer-based hybrid materials starting from an aluminosilicate source (*i.e.* metakaolin, MK), a silicate solution and a low-cost commercial oligomeric siloxane mixture. These new materials can be considered as hybrids of Class II (Kickelbick, [1]) since no phase separation up to nanometric level was detected, indicating a very close interaction between the components, and even

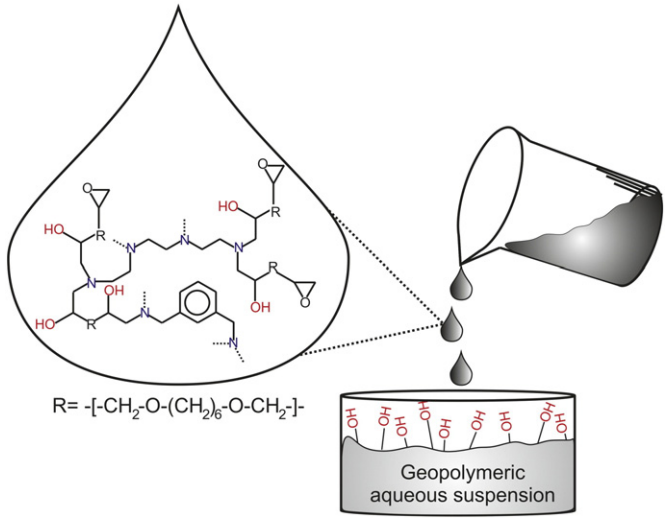

Fig. 1. Schematic representation of the addition of a partly reticulated epoxy resin to the geopolymeric aqueous mixture [24]. Some hydroxyl groups of the organic and inorganic components are highlighted.

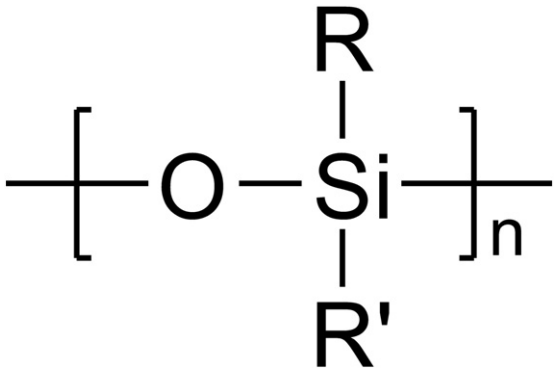

Fig. 2. Chemical structure of a polysiloxane repeating unit.

the likely formation of chemical bonds between geopolymeric and polysiloxane units. It is worth pointing out that, although similar hybrid materials can be obtained through *sol–gel* method [28–32], they are more expensive, requiring pure reagents, an accurate control of the conditions of preparation and the use of organic solvents, hardly suitable for large-scale production.

Besides the synthesis procedure, a detailed analysis of the microstructure of this new material, performed by SEM microscopy, MAS-NMR spectroscopy and X-ray diffraction, is presented. In addition, mechanical, thermal as well as some functional properties (such as fire resistance) of such hybrid materials are also investigated and compared with those of geopolymer composites prepared by the same synthetic approach and containing the same content of an organic (epoxy) component [24].

2. Experimental

2.1. Materials

A commercial oligomeric dimethylsiloxane mixture was purchased from Globalchimica S.r.l. with the name of Globasil AL20 while the Sn(IV) catalyst, named Rhodosil Catalyseur PC Thixo was purchased from Bluestar Siliconi Italia S.p.a.. The commercial name of the silicone rubber produced by reaction of the used oligomeric dimethylsiloxane mixture catalyzed by the Sn(IV) complex is RTV3330®. Sodium hydroxide, reagent grade, was supplied by Aldrich. Metakaolin, supplied by Neuchem S.r.l. (Milan, Italy), has the composition reported in Table 1. The sodium silicate solution was supplied by Prochin Italia S.r.l. with the composition reported in Table 1.

2.2. Preparation of polydimethylsiloxane

Polydimethylsiloxane (PDMS) samples were prepared by adding a Sn(IV) based catalyst at 5% by weight to the commercial oligomeric dimethylsiloxane mixture at room temperature. The polymerization reaction was carried out at room temperature (≈25 °C) for 12 h.

Table 1
Chemical composition (wt.%) of the metakaolin and of the sodium silicate solution.

Metakaolin							
Al_2O_3	SiO_2	K_2O	Fe_2O_3	TiO_2	MgO	CaO	Others
41.90	52.90	0.77	1.60	1.80	0.19	0.17	0.67

Sodium silicate solution		
SiO_2	Na_2O	H_2O
27.40	8.15	64.45

2.3. Preparation of geopolymer

The alkaline activating solution was prepared by dissolving solid sodium hydroxide into the sodium silicate solution. The solution was then allowed to equilibrate and cool for 24 h. The composition of the solution can be expressed as Na_2O $1.4SiO_2$ $10.5H_2O$. Then metakaolin was incorporated into the activating solution with a liquid to solid ratio of 1.4:1 by weight, and mixed by a mechanical mixer for 10 min at 800 rpm. As revealed by EDS analysis on the cured samples, the composition of the whole geopolymeric system can be expressed as Al_2O_3 $3.5SiO_2$ $1.0Na_2O$ $10.5H_2O$, corresponding to a complete geopolymerization process.

2.4. Preparation of hybrid samples

Hybrid polysiloxane–geopolymer samples were prepared by incorporating the commercial oligomeric dimethylsiloxane mixture, according to different weight contents, into the freshly prepared geopolymeric suspension under mechanical stirring, when the polycondensation reaction of both geopolymer and dimethylsiloxane was already started but far to be completed. In particular, in order to promote the polycondensation of dimethylsiloxane units to PDMS, a catalytic amount of the commercial Sn(IV) catalyst was added in some of the prepared samples to the dimethylsiloxane mixture, few minutes before its mixing with the geopolymeric suspension.

By following this procedure, a set of samples with different w/w ratios, ranging between 5 and 15% of dimethylsiloxane in the geopolymer suspension, were prepared. These samples are hereafter indicated as SiligeoXX, where XX stands for the weight percentage of dimethylsiloxane added to the geopolymer slurry.

An additional set of samples, characterized by the same content of dimethylsiloxane oligomers but obtained without the addition of the Sn(IV) catalyst, was prepared too. These samples are hereafter indicated as SiligeoNCXX, where XX stands again for the weight percentage of dimethylsiloxane oligomer content.

2.4.1. Curing treatments

As soon as prepared, a first set of SiligeoXX and SiligeoNCXX samples was poured in cubic molds and cured in >95% relative humidity conditions at room temperature for seven days and left further 21 days in air at room temperature. A second set of samples was poured in cubic molds, cured in the same relative humidity conditions at 60 °C for 48 h and then kept still in >95% relative humidity conditions at room temperature for further 5 days. Afterwards, the specimens were kept further 21 days in air at room temperature. The suffix -RT or -T60 has been added to the name of the specimen to indicate their curing at room temperature or at 60 °C, respectively. For all the samples, the evaporation of water was prevented by sealing the top of the molds with a plastic film during the curing stage.

In the following sections, the structure and the properties of the Siligeo and SiligeoNC samples are compared with those of the hybrid composite specimens prepared by means of the same experimental procedure but using a commercial epoxy resin (hereafter indicated as GeoepojetXX, where XX refers to the weight percentage of epoxy resin used in the sample preparation) [24]. The comparison is also conducted referring to samples of neat geopolymer prepared and cured in the same experimental conditions.

2.5. Experimental methods

SEM analysis was carried out by means of a FEI Quanta 200 FEG microscope. EDS analyses were performed by using an Energy Dispersive Spectrometer Oxford Inca Energy System 250 equipped with an INCAx-act LN2-free detector at 20 kV. SEM specimens were gold coated before the analysis.

Solid-state magic-angle-spinning nuclear magnetic resonance spectroscopy (SS MAS-NMR) experiments were performed at room temperature using a Bruker Avance 300 spectrometer operating at 59.6 MHz. ^{29}Si spectra were recorded with a pulse width and recycle delay of 5.5 μs and 5 s, respectively. The samples, after grinding, were loaded in 7 mm zirconia rotors and spun at 4 kHz. The number of collected transient is 1000. Deconvolution procedures were carried out using the solid lineshape analysis tool of MestreNova with Gaussian peaks, line widths and intensities of all peaks were free to be altered by the optimization independently, but no Lorentzian character was allowed.

Wide-angle X-ray diffraction patterns were obtained at room temperature with nickel-filtered Cu Kα radiation with an automatic Philips powder diffractometer operating in the θ/2θ Bragg–Brentano geometry using a specimen holder of thickness equal to 2 mm.

Uniaxial compressive tests were carried out on $4 \times 4 \times 4$ cm^3 cubic specimens by means of a MTS 810 servo-hydraulic universal testing machine. For each sample type, three specimens were tested under displacement control in order to obtain the corresponding stress–strain curve, compressive strength and Young's modulus. The compressive tests were performed until the sample ruptured at a constant displacement velocity of 0.60 mm/min. The measurement of the displacement was given by the crosshead displacement while the Young's modulus of each sample was computed from the linear stress–strain response recorded during the test. All values presented in the current work were an average of three samples, with the error reported as standard deviation from mean value.

The pore size distribution and the density of the specimens were determined by means of mercury intrusion porosimetry (MIP) using Thermo Pascal 140 and 440 (Thermo Scientific, Milan, Italy).

Flame tests were performed by means of a cone calorimeter in accordance with the procedure described in the ISO5660 standard method. The heat flux produced was 50 kW/m^2 on the specimen, which had an exposed surface of 100 × 100 mm. The testing equipment consisted of a radiant electric heater in trunk-conic shape, an exhaust gas system with oxygen monitoring and instrumentation to measure the gas flux, an electric spark for ignition, and a load cell to measure the weight loss. The test was terminated after 600 s of exposure.

Heat treatments on specimens have been performed by using a Neytech 15P muffle. The samples were heated from room temperature to 800 °C in air, at a heating rate of 20 °C/min.

3. Results and discussion

3.1. Structural characterization

In Fig. 3, SEM images of fresh fracture surfaces of Siligeo10 samples, *i.e.* prepared by mixing the geopolymeric suspension with 10% w/w of the dimethylsiloxane precursors, are compared with those of Geoepojet10 composite obtained through the same experimental procedure by adding a commercial epoxy resin [33].

The morphologies of the two samples appear completely different. First of all, in all examined Siligeo samples no microcracks are detectable, showing a very compact structure.

Furthermore, while in the Geoepojet10 composite sample (Fig. 3A′) the organic resin is segregated in well-defined microspheres (having diameters in the range of 1–20 μm), in the Siligeo10 sample (Fig. 3A) it is possible to recognize only one phase, even at nanometric level scale as discussed later in more detail. The different morphologies are also highlighted by EDS analyses, presenting a very different distribution of silicon and carbon atoms in Siligeo10 (Fig. 3B–C) and Geoepojet10 (Fig. 3B′–C′) specimens.

In fact, while in the Geoepojet10 composite, carbon atoms (Fig. 3C′) are mostly segregated in spherical regions corresponding to the organic particles (well visible in Fig. 1A′) and Si atoms (Fig. 3B′) are mostly concentrated in the geopolymeric matrix, in the Siligeo10 specimen, a continuous distribution of silicon (Fig. 3B) and carbon (Fig. 3C) in the

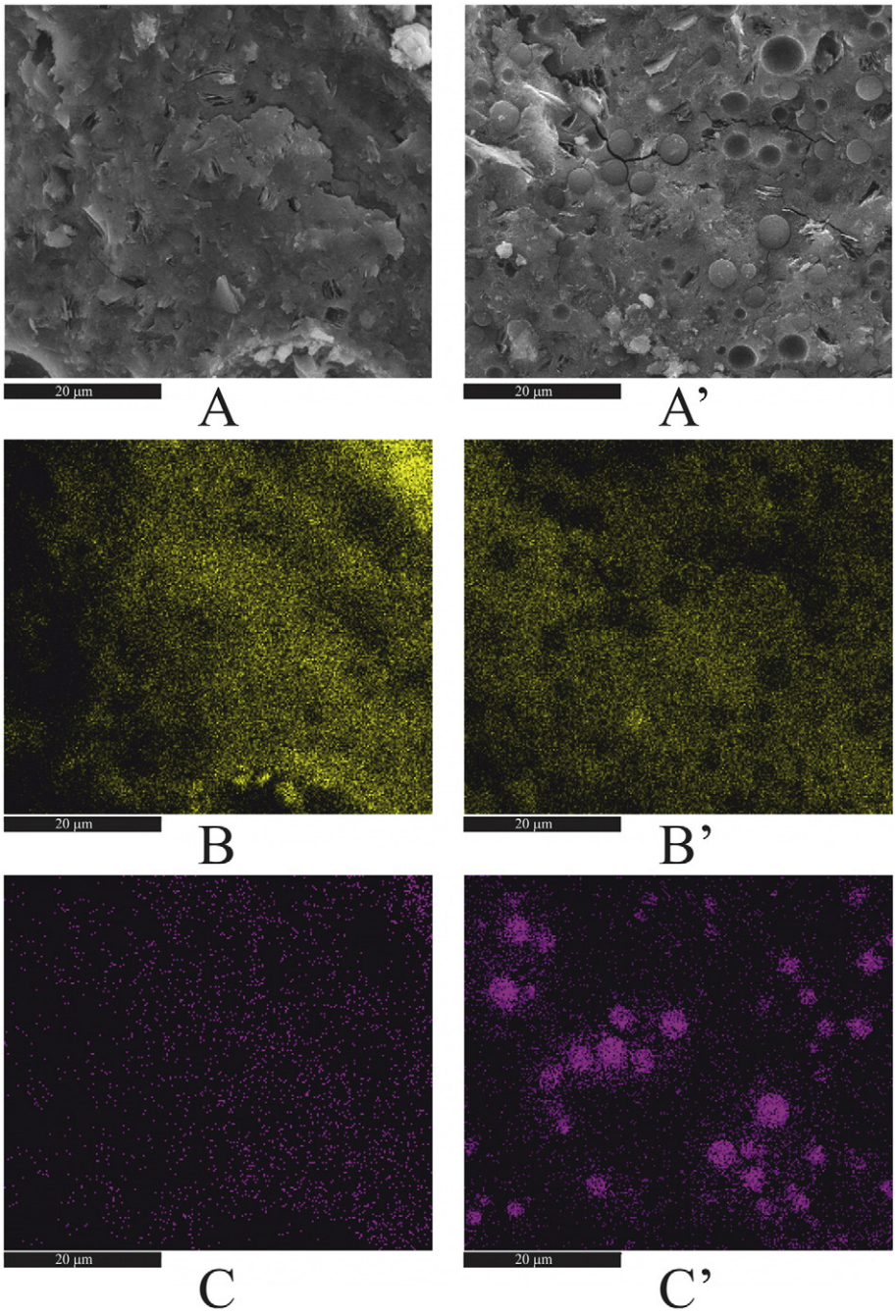

Fig. 3. SEM images at 5,000 magnifications (A, A′) and EDS maps at the same magnification of the elements silicon (B, B′) and carbon (C, C′) in the Siligeo10 (A, B, C) and the Geoepojet10 sample (A′, B′, C′), respectively.

overall surface is present. These data highlight that, in the case of Geoepojet10, phase segregation between the organic and inorganic domains takes place [24], while as for Siligeo10 specimen, a sort of interpenetrated network between the geopolymeric and siloxane components is likely to have been created, in which chemical bonds between the aluminosilicate and siloxane components could be present.

A schematic representation of a possible crosslink between the reactive geopolymeric mixture and the dimethylsiloxane oligomeric mixture taking place during the formation of the hybrid material is shown in Fig. 4.

Due to the similarity of the microstructure of Siligeo10 specimen to that of a neat geopolymer, a more detailed investigation was carried out. Fig. 5 shows SEM images at 50,000 and 100,000 magnifications for a neat geopolymer, Siligeo10 and SiligeoNC10 specimens. The morphology of the neat geopolymer (Fig. 5A, B) could be described as a three-dimensional network, characterized by the presence of very small voids (with an average diameter of less than 20 nm), representing a diffuse not interconnected nanoporosity. This morphology could be attributed to the geopolymerization process. In fact, it is well known that, when the geopolymeric reactive suspension is obtained by mixing an aqueous solution of sodium silicate and sodium hydroxide with metakaolin, the latter is hydrolyzed by the alkaline environment, producing aluminate and silicate species [4]. Accordingly, a complex mixture of silicate, aluminate and aluminosilicate species is formed and a complex equilibrium between them is established [34]. In this strongly alkaline environment, the geopolymerization reaction proceeds leading to the formation of a gel due to the condensation of the oligomers into a large network. After gelation, the system continues to

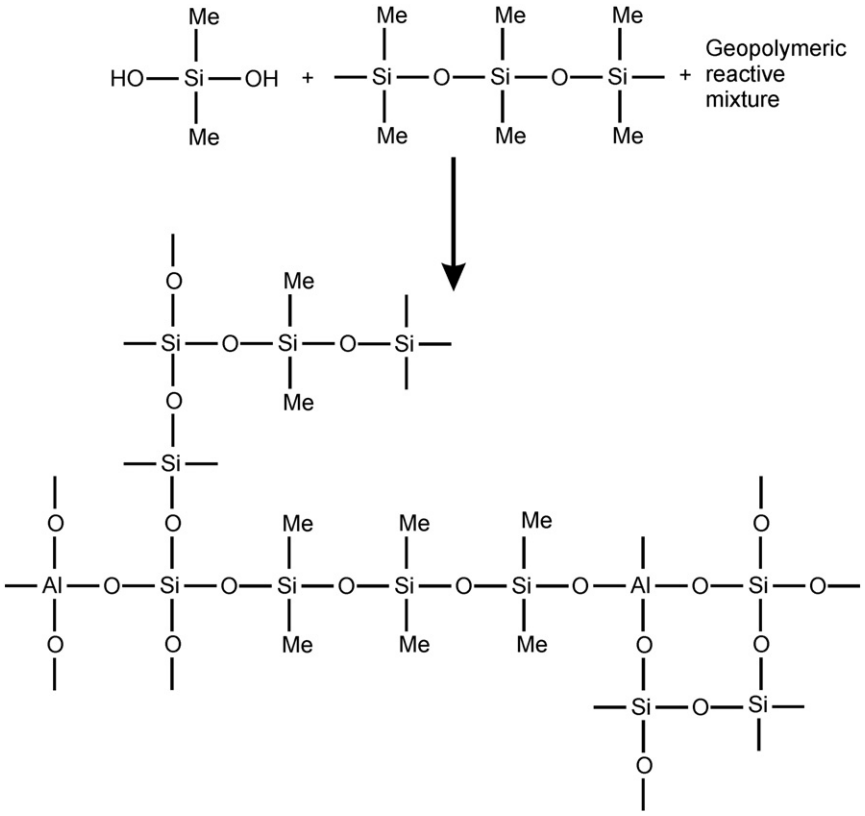

Fig. 4. Schematic representation of a possible bonding formation between siloxane and aluminosilicate units during the simultaneous dimethylsiloxane–geopolymer polycondensation process leading to Siligeo hybrid material.

rearrange and reorganize itself, affording a three dimensional aluminosilicate network consisting of alternating Si and Al tetrahedra which share oxygen atoms and in which the alkali cations compensate the charge associated with the tetrahedra of Al [4,35]. According to this description, the observed nanoporosity (Fig. 5B) could be attributed to the removal of water molecules during the curing process leading to the geopolymer [36,37]. In the case of SiligeoNC10 sample (Fig. 5C), the observed morphology is very different in respect to that of the neat geopolymer since it appears to be more compact, characterized by the presence of nodules with an average diameter of about 40–50 nm while no diffuse porosity is present (Fig. 5D).

By examining Siligeo10 sample at 50,000 magnifications (Fig. 5E), a more uniform morphology appears and no evident granules are detectable while a compact, granular structure, very similar to that observed in the case of SiligeoNC10 (Fig. 5D) is evident also for this sample when examined at even higher magnifications (Fig. 5F).

It is worth pointing out that, in the case of Siligeo10 specimen, in some areas (top left of Fig. 5E), it is possible to observe the presence of concretions that could be attributable to PDMS rubber particles. The occurrence of these particles is probably due to the fact that in the presence of the catalyst, a competition between the reactions of the formation of polydimethylsiloxane and the formation of the hybrid material can occur. Indeed, the Sn(IV) catalyst could allow the formation of very small domains of PDMS dispersed in the bulk. In the absence of the catalyst (SiligeoNC10), instead, the polycondensation of polysiloxane in the strongly alkaline environment is not favored and it does not compete with the simultaneous polymerization and formation of chemical bonds between geopolymeric and siloxane units. Although the microstructures of the two types of hybrid samples (Siligeo and SiligeoNC) comprehensively appear very similar, the corresponding mechanical performances (see Section 3.2.1) seem to be affected by the presence of the catalyst.

A further evidence of the formation of a hybrid material in the case of the Siligeo samples was achieved by examining the morphology of the specimens after thermal treatment at 800 °C in air for 12 h. This additional treatment was aimed at removing the organic moieties from the samples, allowing a better understanding of the resultant microstructure. In the case of heat treated Geoepojet10 specimen, a porous structure attributed to the removal of the organic resin spheres was observed (Fig. 6A), while heat treated Siligeo10 sample still showed a uniform structure (Fig. 6B). By examining the material in more detail (Fig. 6C), it is possible to point out that the thermal treatment at 800 °C produces a change in the nodular morphology observed in the untreated Siligeo10 sample and the development of well-formed crystalline domains. This is in agreement with the X-ray diffraction patterns shown in Fig. 7, confirming the development of a crystalline phase after the thermal treatment at high temperature of the initially amorphous Siligeo specimens. It is worth pointing out that the development of a crystalline phase has been already observed also for heat treated neat geopolymers [38] and organic–inorganic geopolymer based composites [24].

Siligeo10 and SiligeoNC10 cured at different temperatures were characterized also by ^{29}Si MAS-NMR spectroscopy along with the reference neat geopolymer. ^{29}Si MAS-NMR experiments allow the identification of the types and the relative amount of the different $SiQ^n(mAl)$ (where $0 \le m \le n \le 4$, n is the coordination number of the silicon center; m is the number of Al neighbors) structural units of geopolymers and, at the same time, the structural changes during the polymerization [4,39]. Accordingly, ^{29}Si MAS-NMR analyses were used to identify the microstructural changes occurring as a consequence of both the thermal curing and the addition of the dimethylsiloxane units to the geopolymer mixture, while its polycondensation was still taking place.

Fig. 8 shows the ^{29}Si NMR spectra of a neat geopolymer, a SiligeoNC10 and a Siligeo10 sample cured at room temperature ($\approx$25 °C) and at 60 °C.

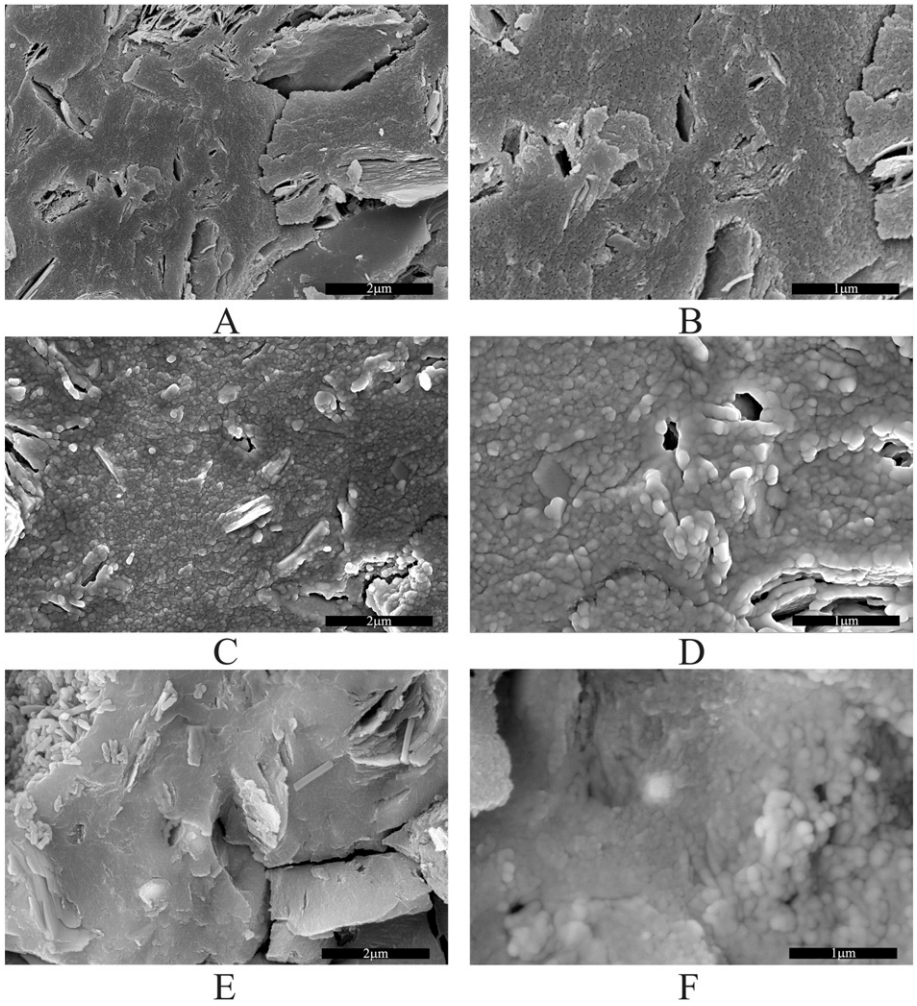

Fig. 5. SEM images at 50,000 (A, C, E) and 100,000 (B, D, F) magnifications of geopolymer-RT (A, B), SiligeoNC10-RT (C, D) and Siligeo10-RT (E, F) specimens.

It is well known that geopolymers are characterized by a three dimensional cross-linked structure, mainly consisting of Q^4 and Q^3 units. Spectrum a of Fig. 8A, referring to neat geopolymer-RT, shows a single broad resonance, characteristic of an amorphous material and containing a range of slightly different environments. This resonance is centered at −92.1 ppm, and could be attributable to $Q^4(2Al)$ or to the convolution of different ^{29}Si environments, such as $Q^4(1Al)$ (−91 ppm and −96 ppm) [40,41].

In the spectrum of the neat geopolymer-T60, the same single broad resonance is present, although slightly shifted to more negative chemical shifts (−93.1 ppm, lower frequencies of the field). This shift could be attributed to a higher degree of polymerization of the samples cured at higher temperatures, resulting in an increase of the nominal Si/Al ratio in the specimens attributed to replacement of aluminum first cation neighbors with silicon more shielding nucleus [42–45].

A similar shift of the signal towards lower frequencies with the increase of the curing temperature is reordered also in Siligeo and SiligeoNC samples (see, in Fig. 8A, spectrum b (−93.1 ppm) *vs* spectrum a (−92.1 ppm); spectrum d (−93.9 ppm) *vs* spectrum c (−92.7 ppm); spectrum f (−94.9 ppm) *vs* spectrum e (−92.1 ppm)).

These shifts, indicating an increase of the nominal Si/Al ratio, are also noticeable by comparing NMR spectra of the neat geopolymer with those of Siligeo and SiligeoNC specimens cured in the same conditions. In particular, SiligeoNC-T60 NMR spectrum presents the greatest shift since its broad peak is centered at −94.9 ppm (Fig. 8C) compared to −92.1 and −93.1 ppm of neat geopolymer and geopolymer-T60, respectively.

This result could indicate that the samples obtained in the absence of catalyst present a higher silicon content incorporated in the three-dimensional network, supporting the hypothesis of a bonding interaction between the silicon atoms deriving from the dimethylsiloxane units and those deriving from metakaolin and from the silicate solution.

Siligeo and SiligeoNC spectra show a resonance attributable to PDMS (whose ^{29}Si spectrum is shown in Fig. 8A-g) since dimethylsiloxane monomers and oligomers are able to polymerize also in the alkaline environment of the geopolymerization reaction, independently of the presence of the Sn(IV) catalyst (Fig. 8A, spectra c–f). It is interesting also to note that, in the SiligeoNC10 samples, this resonance appears smaller and broader in respect to the same signal recorded in the case of the Siligeo10 samples (Fig. 8B). This broadening is plausibly due to the intimate mixing of siloxane units with the geopolymer precursors. Indeed, while in the case of commercial PDMS the silicon peak is sharp, evidencing an ordered sequence of repetitive groups, in the case of the PDMS formed in the hybrid samples, this resonance appears to be broader, accounting to some extents for the occurrence of chemical bonds between the siloxane units and the amorphous geopolymer [46]. Furthermore, in the case of SiligeoNC10-T60 specimen, the presence of an additional peak at −31 ppm, could be the evidence of a different chemical environment experienced by the silicon in the Me_2Si units.

Another evidence indicating a good dispersion and bonding interaction between silicon precursor and geopolymer network in the case of SiligeoNC10-T60 specimen, could be represented by the reduced intensity of the resonance attributable to PDMS terminal

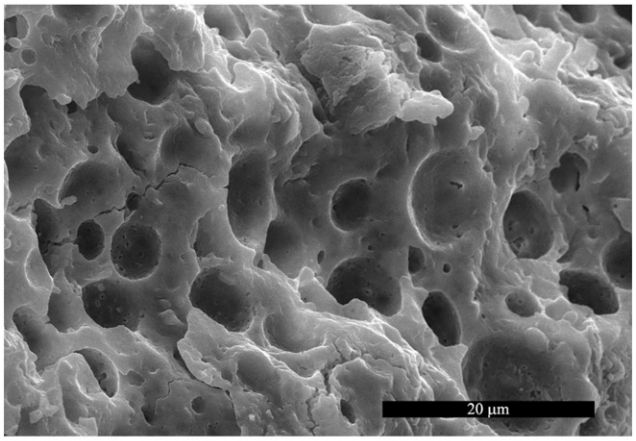

A

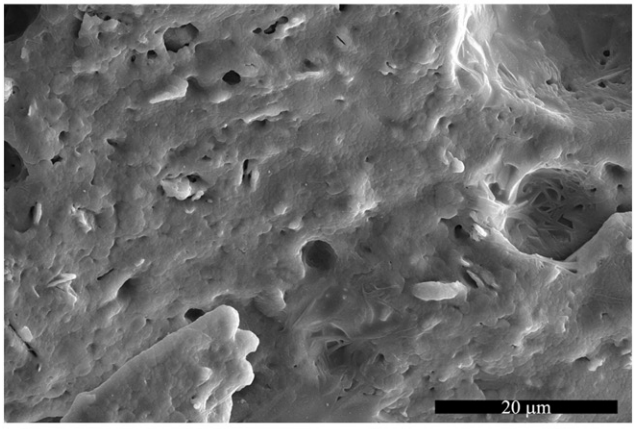

B

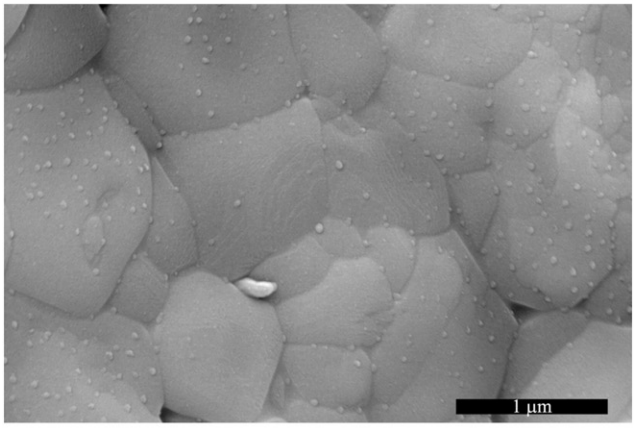

C

Fig. 6. SEM images at 5,000 (A, B) and 100,000 (C) magnifications of Geoepojet10-RT (A) and Siligeo10-RT (B, C) specimens cured at room temperature after their heat treatment in air at 800 °C for 12 h.

groups [–Si$(CH_3)_3$] at 4 ppm in the ^{29}Si spectrum (Fig. 8A-e, f) in respect to the well detectable signal characterizing the spectra of the samples prepared by adding also the catalyst to the polymerizing mixture (Fig. 8A-c, d). This reduction is apparent also from the deconvolution of the spectra reported in Table 2.

All the discussed evidences concerning the chemical structure support the hypothesis that SiligeoNC10-T60 represents the sample in

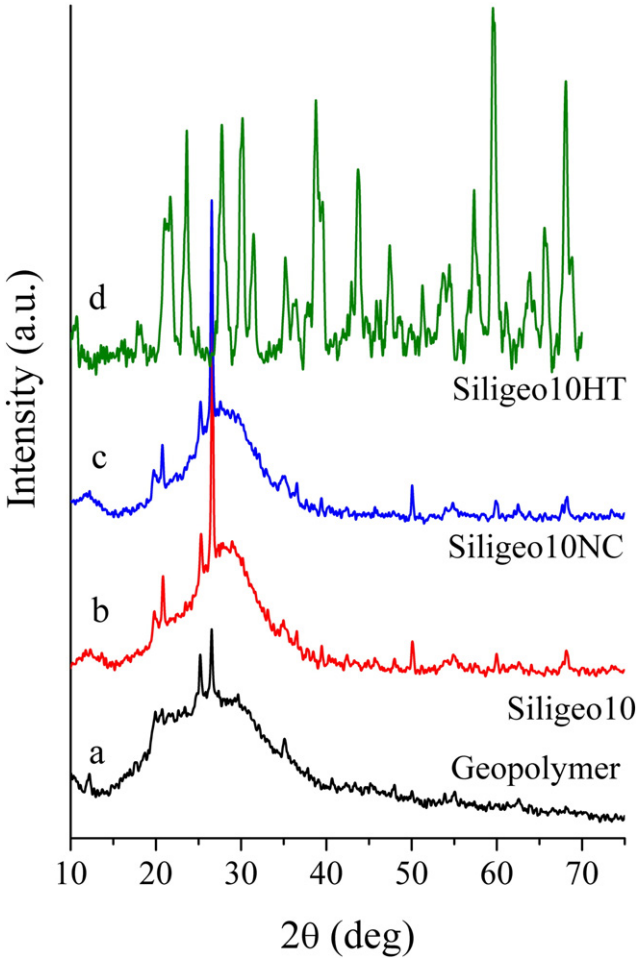

Fig. 7. X-ray diffraction patterns of geopolymer (a), Siligeo10-T60 (b), SiligeoNC10-T60 (c) and Siligeo10-T60 specimens after the thermal treatment at 800 °C in air for 12 h (Siligeo10HT, label d). The crystalline phase developed in d is nepheline.

which the best chemical interaction between the two initial components was achieved.

3.2. Physico-chemical characterization of hybrid samples

Siligeo and SiligeoNC physico-mechanical properties were characterized by means of several techniques. In particular, the mechanical properties, the porosity and fire resistance were studied and discussed in this section.

3.2.1. Compressive behavior

As far as mechanical properties are concerned, the results of uniaxial compressive tests carried out on Siligeo and SiligeoNC, the average values of compressive strength and Young's modulus (on three samples) are shown in Figs. 9 and 10. In order to point out the effect of dimethylsiloxane oligomer content and curing conditions on the mechanical properties of the specimens, several samples were also tested, differing in dimethylsiloxane oligomer content (ranging from 5 to 15 wt.%) and curing temperature (T = 60 °C or room temperature — RT, ≈25 °C). For comparison purposes, the same tests were performed also on neat geopolymer and Geoepojet samples, prepared and cured in the same experimental conditions.

As far as compressive strength is concerned (Fig. 9), the neat geopolymer and the Geoepojet samples reported an average value of 47 ± 7 and 41 ± 4 MPa, respectively. For Siligeo and SiligeoNC specimens, both dimethylsiloxane content and curing conditions demonstrated to have significant influence on compressive strength. In

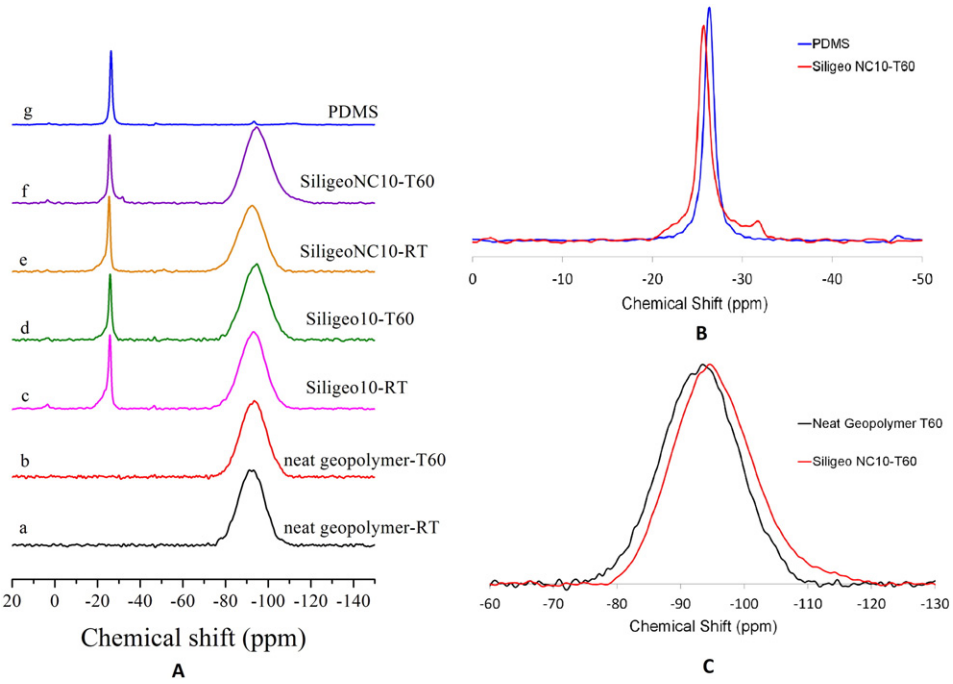

Fig. 8. (A) ^{29}Si MAS-NMR spectra of a neat geopolymer-RT (a); neat geopolymer-T60 (b); Siligeo10-RT (c); Siligeo10-T60 (d); SiligeoNC10-RT (e); and SiligeoNC10-T60 (f). The ^{29}Si NMR spectra of PDMS rubber obtained by polymerization of the oligomeric siloxane mixture catalyzed by Sn(IV) catalyst are shown for comparison (g). Enlarged areas (B, C).

particular, the greatest increase in compressive strength (up to 40% than the neat geopolymer) was achieved in the cases of dimethylsiloxane contents of 5 and 10 wt.%, with the latter case that experienced a less remarkable dependence on the curing/synthesis conditions. On the contrary, for higher dimethylsiloxane content (15 wt.%), the resulting compressive strength was significantly improved in respect to the reference geopolymer only in the case of SiligeoNC15-T60 while in the cases SiligeoNC15-RT, Siligeo15-RT and Siligeo15-T60, the resulting compressive strengths remained almost unchanged or even lowered. It is worth noting that, for each Siligeo and SiligeoNC composition, the highest value of the average compressive strength was achieved when samples were cured at T = 60 °C (green bars); under these conditions, compressive strength was always greater than that recorded for neat geopolymer. Moreover, by comparing the mechanical performances of Siligeo and SiligeoNC specimens with the same composition and cured in the same experimental conditions (*i.e.* keeping the curing temperature at 60 °C), it is noticeable that the addition of Sn(IV) based catalyst (red bars) led to a slight reduction in the compressive strength enhancement in respect to the SiligeoNC specimens. When SiligeoNC and Siligeo samples were cured at room temperature (blue and pink bars, respectively), an improvement in the compressive strength of the specimens was achieved only for a dimethylsiloxane content equal to 10 wt.%.

Stress–strain curves obtained by compressive tests allowed determining also the Young's modulus of all samples (Fig. 10). Both references, neat geopolymer and Geoepojet10, exhibited a very similar elastic stiffness with a Young's modulus value of approximately equals 2.6 ± 0.5 GPa. In the case of hybrid samples, the overall trend of the results as a function of composition and synthesis/curing conditions, resulted very similar to the one observed for the compressive strength. In particular, the highest increase of Young's modulus was obtained for dimethylsiloxane contents equal to 5 wt.% and 10 wt.%: in the case of SiligeoNC10-T60 sample this increase was even 65% greater than the reference geopolymer. In general, the use of the catalyst and the curing at room temperature reduced the increase of the Young's modulus compared to that achieved by SiligeoNC10-T60; indeed, lower values than neat geopolymer were recorded in some cases (*i.e.* Siligeo5 and Siligeo15).

Because of the large number of specimens tested, only the representative stress–strain curves of the samples that exhibited the best mechanical performance are reported in Fig. 11, along with the curves of the neat geopolymer and Geoepojet10.

The compressive behavior of neat geopolymer and Geoepojet10 resulted very similar in terms of both stiffness and peak of compressive stress. In the case of geopolymer, the failure stress was poorly defined and characterized by subsequent loading drops next to the final and complete loss of load carrying capacity at relatively high failure strains. On the contrary, Geoepojet10 exhibited a smoother behavior next to the ultimate failure, resulting in an increased toughness [26]. With regard to SiligeoNC10, all curves exhibited a well defined elastic regime, already visible at the early stages of stress, with a remarkable much stiffer compressive response compared to reference samples. The linear elastic regime remained with an almost constant slope until the ultimate collapse characterized by a sharp peak on the stress strain curve was reached. The different synthesis/curing conditions had a slight influence on the elastic stiffness of the SiligeoNC10 and mainly affected the early stages of compressive stress: the greatest improvement in the mechanical performance was provided by SiligeoNC10-T60, whereas a slightly

Table 2
Relative intensity (%) of the resonance attributable to neat geopolymer and Siligeo (signal at ≈−100 ppm) and polydimethylsiloxane (PDMS, signal at ≈−26 ppm) specimens obtained from the deconvolution procedure of the ^{29}Si spectra reported in Fig. 8. The intensity of the resonance that can be ascribed to PDMS terminal groups [–Si(CH$_3$)$_3$] at 4 ppm is also reported.

Sample	Geopolymer (%)	PDMS (%)	PDMS terminal groups (%)
a	100.00	–	–
b	100.00	–	–
c	84.96	15.03	0.74
d	85.60	12.40	0.37
e	82.86	17.15	0.22
f	87.45	12.55	0.17
g	–	96.60	1.84

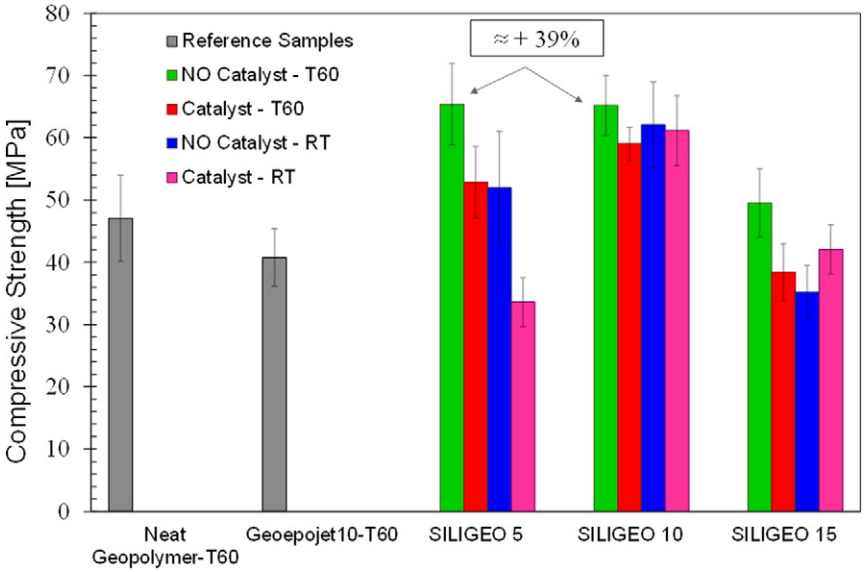

Fig. 9. Average compressive strength for the reference samples (*i.e.* neat geopolymer and Geoepojet10 with gray bars), Siligeo without catalyst and cured at T = 60 °C (green bars) or at room temperature (blue bars), Siligeo with catalyst and cured at T = 60 °C (red bars) or at room temperature (pink bars). Siligeo and SiligeoNC samples have been grouped according to the wt.% of dimethylsiloxane content.

less stiff response was obtained in the case of SiligeoNC10 cured at room temperature.

The observed mechanical behavior suggests some important considerations on the relationship between microstructure and mechanical properties of the hybrid samples, also considering the results discussed in previous paragraphs. It is recognized that the physical and mechanical properties of geopolymer-like materials strongly rely on the composition, degree of geopolymerization and microstructure, with the latter significantly affecting the elastic modulus in compression [47,48]. From the point of view of a mechanics interpretation, in the case of Geoepojet10, the heterogeneous microstructure, characterized by microdispersion of well-defined organic particles into the inorganic matrix (typical of a composite material), did not trigger an appreciable increase of the Young's modulus as the (hardened) resin phase is characterized by a value of the Young's modulus very similar to that of the neat geopolymer (around 2.5 GPa). In this case, the mechanical effect could be rather a toughening mechanism (with regard to fracture) due to the presence of the resin which reduces the void/pore content (Fig. 12C) and, consequently, the cracking initiation sites as approaching the collapse stress [26] (Fig. 11). By keeping the assumption of an heterogeneous microstructure (composite) also for Siligeo and SiligeoNC, simple analytical considerations of micromechanics would suggest a decrease in the Young's modulus as the hypothetical silicone rubber phase (at variance with the micro-spheres of epoxy resin in the Geoepojet specimen) would be characterized by an elastic stiffness significantly lower than the one of the neat geopolymer (≪100 MPa). On the contrary, the increase of the Young's modulus (and compressive strength, too) recorded for SiligeoNC10-T60 would suggest the formation of a

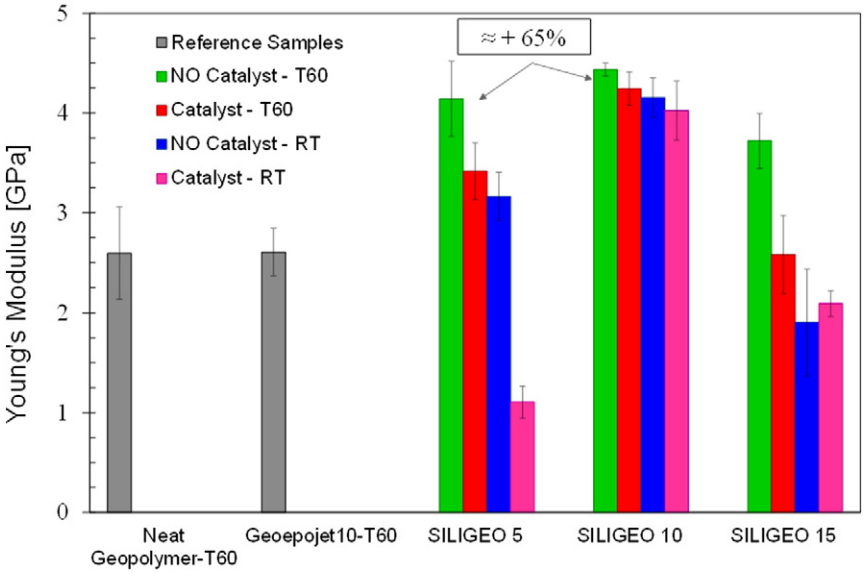

Fig. 10. Average Young's modulus for reference samples (*i.e.* neat geopolymer and Geoepojet10 with gray bars), Siligeo without catalyst and cured at T = 60 °C (green bars), Siligeo with catalyst and cured at T = 60 °C (red bars), Siligeo without catalyst and cured at room temperature (blue bars), Siligeo with catalyst and cured at room temperature (pink bars). Siligeo and SiligeoNC specimens are grouped according to the wt.% of dimethylsiloxane content.

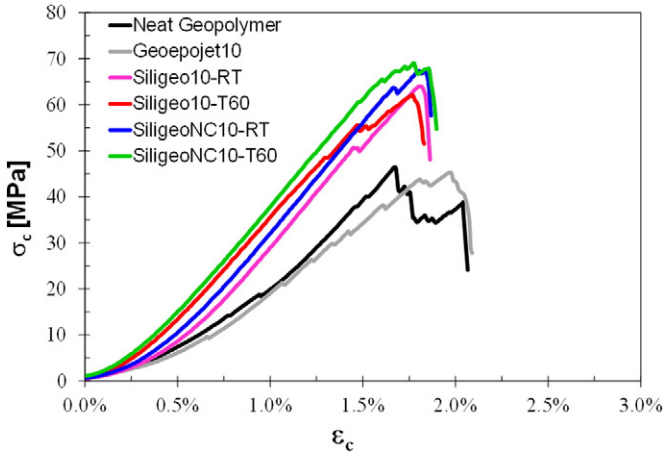

Fig. 11. Compressive stress (σ_c) *vs* strain (ε_c) curves for reference samples (*i.e.* neat geopolymer and Geoepojet10 with black and gray lines. respectively), Siligeo without catalyst and cured at T = 60 °C (green line), Siligeo with catalyst and cured at T = 60 °C (red line), Siligeo without catalyst and cured at room temperature (blue line), Siligeo with catalyst and cured at room temperature (pink line).

stiffer interpenetrated network of aluminosilicate and dimethylsiloxane units rather than a dispersion of discrete silicone particles into a pure geopolymeric matrix.

This interpretation can be also analyzed in light of the mechanical results obtained by varying composition and curing/synthesis methods. As discussed in the NMR section, it is plausible that there might be two concurrent mechanisms that affect the molecular structure of geopolymeric network during hybrid sample synthesis: *i*) silicone rubber formation and *ii*) interaction between siloxane and geopolymer oligomers. It was shown that the use of Sn(IV) catalyst generally tends to lower both Young's modulus and compressive strength of all hybrid samples, with a more relevant effect at low siloxane unit content and for samples cured at room temperature. This fact confirms that the presence of the Sn(IV) catalyst would lead to the formation of PDMS discrete particles that would increase the defect density (cracking initiation pathways) and consequently would act as softening spots in the geopolymer matrix. On the contrary, when dimethylsiloxane oligomers are added to the polymerizing geopolymeric slurry without catalyst and specimens are cured at a higher temperature, an interpenetrated network with a high geopolymerization degree and characterized by a higher stiffness is obtained. Along with the abovementioned preparation and curing conditions, the formation of such a stiffer interpenetrated network has been found to be influenced by dimethylsiloxane unit content too: in fact, mechanical performance is maximized for a dimethylsiloxane content not higher than 10 wt.%, while higher contents (*e.g.* 15 wt.%) do not produce any beneficial effect because the possible formation of discrete particle would lead to a more heterogeneous microstructure.

3.2.2. Porosimetry

The results of the mechanical characterization were also supported by the pore distribution measurements carried out by means of mercury intrusion porosimetry for neat geopolymer, Geoepojet and SiligeoNC samples. Indeed, it is generally accepted that the stiffness and strength of geopolymer-like materials are fundamentally a function of the form and distribution of void space and porosity [49,9].

Mercury porosimetry data are reported in Fig. 12C, where the cumulative volume of mercury intruded (mm^3/g) *versus* pore radius (nm) curves refer to the reference geopolymer (red line), Geoepojet10 (blue line) and SiligeoNC10-T60 (green line) samples.

As anticipated before, by comparing the high resolution SEM images of the neat geopolymer (Fig. 12A) and Siligeo (Fig. 12B) specimens, one can observe that in the case of the neat geopolymer there is a diffuse

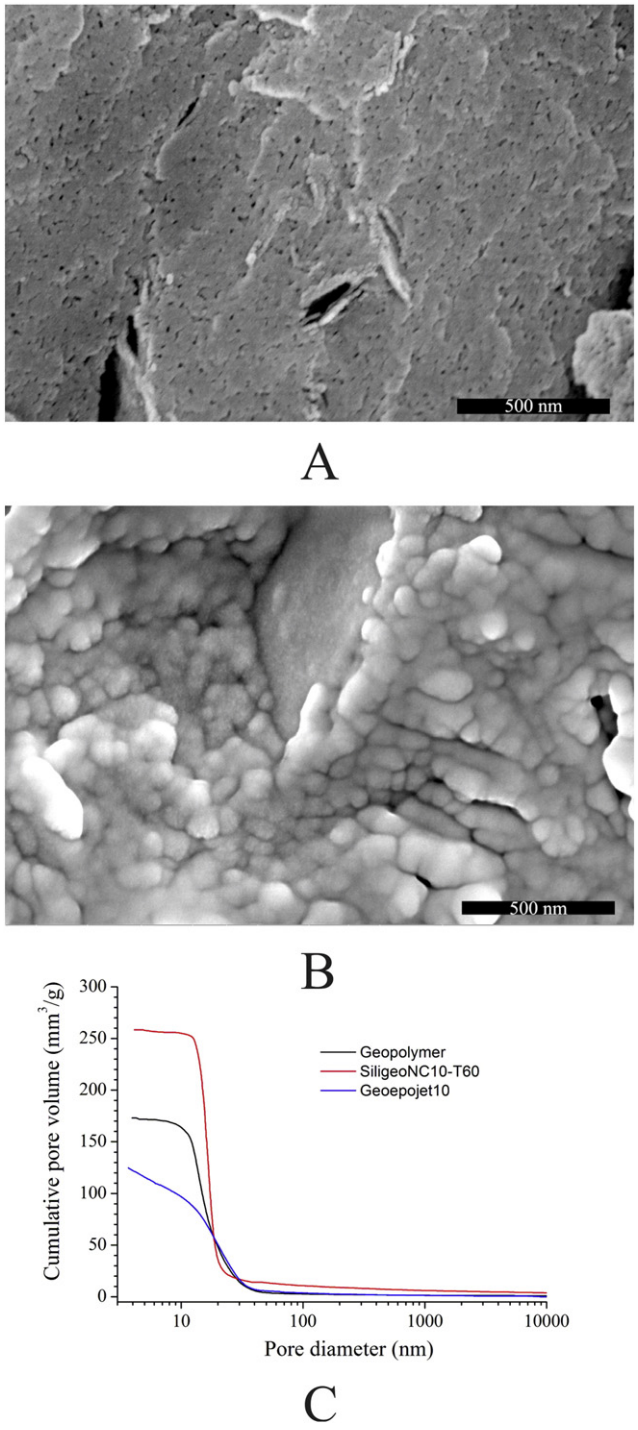

Fig. 12. SEM images at 200,000 magnifications of the neat geopolymer-RT (A) and SiligeoNC10-RT (B) specimens and their cumulative pore volume *vs* pore radius (C) as obtained by mercury intrusion porosimetry analyses. In C the cumulative pore volume curve for the Geoepojet10-RT specimen is reported for comparison.

porosity [50,51] with pore size of a few tens of nanometers, while in the case of Siligeo, small pores are not distinguishable but only large pores (perhaps due to air bubbles that were entrapped during the mixing process and were unable to escape from the samples due to its elevated viscosity) are present. These observations are consistent with the porosimetric curves reported in Fig. 12C.

In the case of the reference geopolymer, it can be observed that most of the nanopores have an average diameter up to 15 nm whereas a

smaller volume is associated to nanopores of maximum 30 nm of diameter. These pores probably resulted from the structural reorganization of the network that led to the expulsion of the water into larger pores in the polycondensation steps. In addition, the total porosity, expressed in terms of cumulative volume of mercury intruded, is approximately ≈ 170 mm^3/g. In the case of the Geoepojet10 composite, the shape of the cumulative pore volume curve changed with respect to the trend observed in the case of the reference geopolymer, showing a wider pore diameter distribution and a reduction of the total pore volume (≈ 120 mm^3/g). On the contrary, SiligeoNC10-T60 exhibited a shape of pore cumulative pore volume curve very similar to the one of neat geopolymer, indicating that the structural arrangement of the nanoscale network was probably kept as the one of reference geopolymer but with stiffer interactions. However, the cumulative pore volume of SiligeoNC10-T60 was ≈ 260 mm^3/g, *i.e.* approximately 50% greater than the reference geopolymer. It has been showed that an increase of pore volume in the microstructure determines a decrease of the mechanical properties of the material whereas a larger gel volume (feature generally found in a more homogenous and less porous microstructure) allows stress during compression to be spread over a larger area, resulting in less strain and higher Young's modulus [9]. However, this circumstance was not confirmed in the case of SiligeoNC10-T60; therefore, mechanical and porosimetry results would suggest that the improvement observed (especially with reference to the Young's modulus) might be linked to the formation of a single and more rigid phase (even though with higher pore volume).

3.2.3. Fire resistance

The cone calorimeter provides important information on the combustion behavior of a material under ventilated conditions. The images of SiligeoNC10 samples before and after the cone calorimeter test are shown in Fig. 13. In the same figure, the images of the reference samples (neat geopolymer and Geoepojet10) are also shown for comparison. As it can be observed for the images, in the case of the neat geopolymer and of the Geoepojet composite specimens, the direct contact with the flame caused the formation of several macroscopic cracks. On the contrary, in the case of the SiligeoNC10 sample, the specimen preserved its structural integrity since only small superficial cracks showed up after the test. Moreover, SiligeoNC10 hybrid sample, despite containing organic moieties, does not show the presence of smoke residuals after the test as reordered in the case of Geoepojet10 composite specimen.

The fire resistance properties are analyzed in more detail by comparing the recorded values of heat release rate (HRR), total heat release (THR), total smoke production (TSP) and smoke production rate (SPR) *vs* time for SiligeoNC10-T60, neat geopolymer, Geoepojet10 and a neat PDMS rubber (Fig. 14) samples [52]. Some significant experimental outcomes referring to these tests are also reported in Table 3.

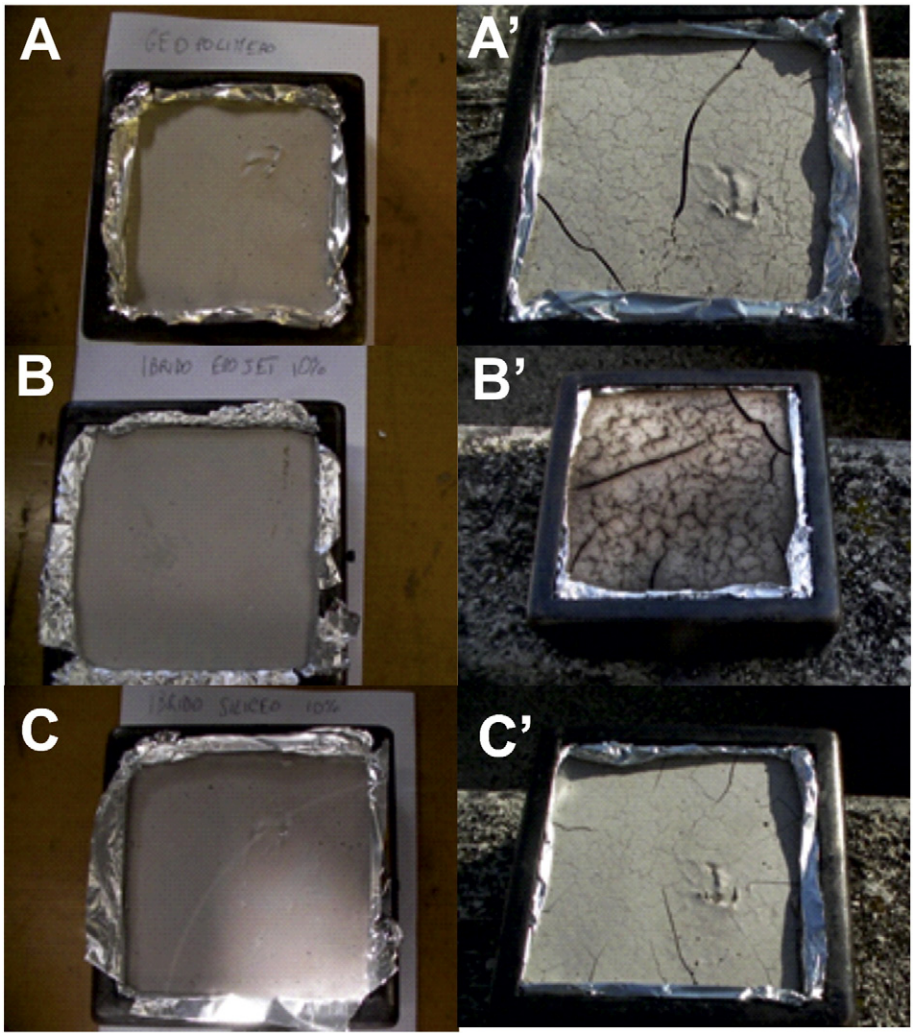

Fig. 13. Neat geopolymer (A, A′), Geoepojet10 (B, B′) and SiligeoNC10 (C, C′) specimens before (A, B, C) and after (A′, B′, C′) the cone calorimeter fire testing.

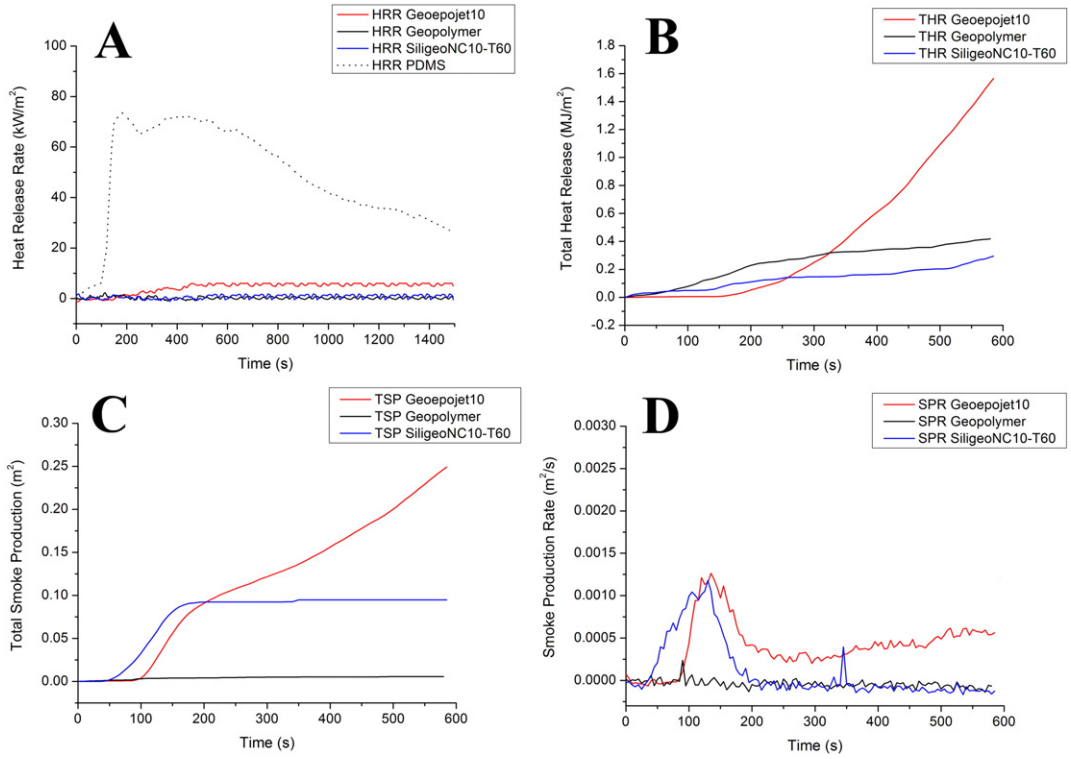

Fig. 14. Selected cone calorimeter test results for neat geopolymer (continuous black line), SiligeoNC10-T60 (continuous blue line), Geoepojet10 (continuous red line) and PDMS rubber (dotted black line): A) HRR (kW/m^2) *vs* time (s); B) total heat release (MJ/m^2) *vs* time; C) total smoke production (m^2) *vs* time (s); and D) smoke production rate (m^2/s) *vs* time (s).

In particular, in the case of the SiligeoNC10-T60, HRR peak rate (that is one of the most important factors to determine the potential behavior of a material during fire) was almost null (Fig. 14A), nearly coincident with that of the neat geopolymer. On the contrary, the neat polydimethylsiloxane (PDMS) sample showed a pronounced HRR increase after few tens of seconds from the start of the test. A similar behavior of SiligeoNC10-T60 and geopolymer can be also pointed out by examining the THR graph (Fig. 14B): in both cases, at variance with the Geoepojet sample that showed an increase of the total heat release *versus* time, their THR values remained practically negligible up to the end of the test. Finally, interesting results were also obtained from the quantification of the smoke generation (Fig. 14C, D) for the Siligeo hybrid material. This sample showed a negligible emission of smokes within the first 3 min of the test (Fig. 14C) that ended up after roughly 1 min (Fig. 14D). At variance, in the case of the Geoepojet10 samples, the combustion of the epoxy resin triggered a more pronounced emission of smokes that increased over time till the end of the test.

Table 3
Selected cone calorimeter test results for neat geopolymer, SiligeoNC10-T60, Geoepojet10 and PDMS rubber: value of heat release rate peak (HRR peak), value of heat release rate at 300 s (HRR 300 s), total heat release at 300 s (THR 300 s) and 600 s (THR 600 s).

Samples[a]	HRR (peak) (kW/m^2)	HRR (300 s) (kW/m^2)	THR (300 s) (MJ/m^2)	THR (600 s) (MJ/m^2)
Neat geopolymer	2.45	0.50	0.29	0.42
Geoepojet10	6.95	0.55	0.25	1.54
SiligeoNC10-T60	3.00	0.23	0.14	0.29
PDMS [52]	74	67	n.a.	n.a.

n.a. = data not available.
[a] For each parameter, the mean value on three independent measurements is reported.

4. Conclusions

New hybrid geopolymer-based materials were prepared through a synthetic approach based on a concurrent polymerization in mild conditions of a commercial oligomeric dimethylsiloxane mixture with an aluminosilicate source (metakaolin) dispersed in a silicate solution.

Microstructural analyses revealed a structural homogeneity of these materials up to nanometric level, suggesting that, thanks to the chemical similarity of the components, strong interactions between siloxane and geopolymeric units can be achieved. ^{29}Si MAS-NMR characterization suggested that the incorporation of siloxane units within the geopolymeric framework depends on the experimental and curing conditions of the samples, being maximized in the case of hybrid samples obtained without the addition of the catalyst used to polymerize dimethylsiloxane monomers and cured at 60 °C. The resultant hybrid structure of these new materials turned out in significantly enhanced compressive strength and stiffness of the samples in respect to those of neat geopolymers and organic–inorganic geopolymer composites. In particular, the mechanical characterization of the samples showed that the optimal performances were recorded for the samples characterized by a dimethylsiloxane unit content of 10 wt.% without the catalyst and cured at 60 °C.

Despite the high content of dimethylsiloxane units in the examined samples (up to 15 wt.%), a good fire resistance of the hybrid material was achieved, significantly higher than that observed in the case of geopolymer based composites with a similar content of fully organic resins and comparable with that of neat geopolymer specimens. This property could be positively exploited in structural applications requiring heat insulation and heat-resistance such as precast concrete panels for the construction industry.

This study demonstrated that, at variance with analogous materials obtained by *sol–gel* approaches (that are much more expensive and require a fine control of the experimental conditions), the discussed

hybrid materials are characterized by a very simple preparation procedure and very interesting technological properties. This suggests also their possible uses even on a large scale, especially for the technological development of alternative geopolymer based binders in the concrete industry. A careful cost analysis needs to be addressed in order to assess the effectiveness of a large scale use of these materials.

Finally, further investigations are needed to tailor the final properties of the hybrid material proposed in the present paper by a suitable selection of the siloxane components and a careful optimization of the production conditions.

Acknowledgments

The authors thank Neuvendis S.p.A. for the metakaolin supply and Prochin Italia S.r.l. for the silicate solution supply.

References

[1] G. Kickelbick, Introduction to hybrid materials, in: G. Kickelbick (Ed.), Hybrid Materials: Synthesis, Characterization, and Applications, Wiley-VCH Verlag GmbH & Co. KGaA, Weinheim, Germany, 2007.
[2] M. Hussain, R. Varely, Y.B. Cheng, Z. Mathys, G.P. Simon, Synthesis and thermal behavior of inorganic–organic hybrid geopolymer composites, J. Appl. Polym. Sci. 96 (2005) 112–121.
[3] K.J.D. Mackenzie, M. Welter, Geopolymer (aluminosilicate) composites: synthesis, properties and applications, in: Woodhead Publishing Limited (Ed.), Advances in Ceramic Matrix Composites, E-Publishing Inc., Cambridge 2014, pp. 445–470.
[4] P. Duxson, A. Fernández-Jiménez, J.L. Provis, Geopolymer technology: the current state of the art, J. Mater. Sci. 42 (2007) 2917–2933.
[5] J. Davidovits, Geopolymer Chemistry and Applications, 3rd ed. Institut Gèopolymère, Saint Quentin, France, 2014 (www.geopolymer.org).
[6] B. Molino, A. De Vincenzo, C. Ferone, F. Messina, F. Colangelo, R. Cioffi, Recycling of clay sediments for geopolymer binder production. A new perspective for reservoir management in the framework of Italian legislation: the Occhito reservoir case study, Materials 7 (2014) 5603–5616.
[7] C. Ferone, B. Liguori, I. Capasso, F. Colangelo, R. Cioffi, E. Cappelletto, R. Di Maggio, Thermally treated clay sediments as geopolymer source material, Appl. Clay Sci. 107 (2015) 195–204.
[8] C. Ferone, F. Colangelo, R. Cioffi, F. Montagnaro, L. Santoro, Use of reservoir clay sediments as raw materials for geopolymer binders, Adv. Appl. Ceram. 112 (2013) 184–189.
[9] J.L. Provis, J.S.J. van Deventer, Geopolymers: Structure, Processing, Properties and Industrial Applications, CRC Press/Taylor and Francis, Boca Raton, FL, USA, 2009.
[10] J. Tailby, K.J.D. MacKenzie, Structure and mechanical properties of aluminosilicate geopolymer composites with Portland cement and its constituent minerals, Cem. Concr. Res. 40 (2010) 787–794.
[11] C. Ferone, F. Colangelo, R. Cioffi, F. Montagnaro, L. Santoro, Mechanical performances of weathered coal fly ash based geopolymer bricks, Procedia Eng. 21 (2011) 745–752.
[12] C. Ferone, F. Colangelo, F. Messina, L. Santoro, R. Cioffi, Recycling of pre-washed municipal solid waste incinerator fly ash in the manufacturing of low temperature setting geopolymer materials, Materials 6 (2013) 3420–3437.
[13] S.F.U. Ahmed, Fibre-reinforced geopolymer composites (FRGCs) for structural applications, in: Woodhead Publishing Limited (Ed.), Advances in Ceramic Matrix Composites, E-Publishing Inc., Cambridge 2014, pp. 471–495.
[14] J. Šesták, N. Koga, P. Šimon, B. Foller, P. Roubíček, N.-L.N. Wu, Amorphous inorganic polysialates: geopolymeric composites and the bioactivity of hydroxyl groups, in: Springer (Ed.), Thermal Analysis of Micro, Nano- and Non-crystalline Materials, E-Publishing Inc. 2013, pp. 441–460.
[15] A. Favier, G. Habert, J.B. d'Espinose de Lacaillerie, N. Roussel, Mechanical properties and compositional heterogeneities of fresh geopolymer pastes, Cem. Concr. Res. 48 (2013) 9–16.
[16] L. Ricciotti, G. Roviello, O. Tarallo, F. Borbone, C. Ferone, F. Colangelo, M. Catauro, R. Cioffi, Synthesis and characterizations of melamine-based epoxy resins, Int. J. Mol. Sci. 14 (2013) 18200–18214.
[17] L. Ricciotti, F. Borbone, A. Carella, R. Centore, A. Roviello, M. Barra, G. Roviello, C. Ferone, C. Minarini, P. Morvillo, Synthesis of highly regioregular poly[3-(4-alkoxyphenyl)-thiophene]s by oxidative catalysis using copper complexes, J. Polym. Sci. A Polym. Chem. 51 (2013) 4351–4360.
[18] Z. Zhang, X. Yao, H. Zhu, S. Hua, Y. Chen, Preparation and mechanical properties of polypropylene fiber reinforced calcined kaolin–fly ash based geopolymer, J. Cent. South Univ. Technol. 16 (2009) 49–52.
[19] Y. Zhang, W. Sun, Z. Li, Impact behavior and microstructural characteristics of PVA fiber reinforced fly ash-geopolymer boards prepared by extrusion technique, J. Mater. Sci. 41 (2006) 2787–2794.
[20] Y. Zhang, W. Sun, Z. Li, X. Zhou, Impact properties of geopolymer based extrudates incorporated with fly ash and PVA short fiber, Constr. Build. Mater. 22 (2008) 370–383.
[21] S. Zhang, K. Gong, J. Lu, Novel modification method for inorganic geopolymer by using water soluble organic polymers, Mater. Lett. 58 (2004) 1292–1296.
[22] Y.J. Zhang, S. Li, D.L. Xu, B.Q. Wang, G.M. Xu, D.F. Yang, N. Wang, H.C. Liu, Y.C. Wang, A novel method for preparation of organic resins reinforced geopolymer composites, J. Mater. Sci. 45 (2010) 1189–1192.
[23] C. Ferone, G. Roviello, F. Colangelo, R. Cioffi, O. Tarallo, Novel hybrid organic–geopolymer materials, Appl. Clay Sci. 73 (2013) 42–50.
[24] G. Roviello, L. Ricciotti, C. Ferone, F. Colangelo, R. Cioffi, O. Tarallo, Synthesis and characterization of novel epoxy geopolymer hybrid composites, Materials 6 (2013) 3943–3962.
[25] F. Colangelo, G. Roviello, L. Ricciotti, C. Ferone, R. Cioffi, Preparation and characterization of new geopolymer–epoxy resin hybrid mortars, Materials 6 (2013) 2989–3006.
[26] C. Ferone, F. Colangelo, G. Roviello, D. Asprone, C. Menna, A. Balsamo, A. Prota, R. Cioffi, G. Manfredi, Application-oriented chemical optimization of a metakaolin based geopolymer, Materials 6 (2013) 1920–1939.
[27] G. Roviello, L. Ricciotti, C. Ferone, F. Colangelo, O. Tarallo, Fire resistant melamine based organic–geopolymer hybrid composites, Cem. Concr. Compos. 59 (2015) 89–99.
[28] E. James, C.Y.-C. Lee, P.A. Bianconi, Hybrid Organic–Inorganic Composites, American Chemical Society, Washington, D.C., 1995
[29] J. Wen, G.L. Wilkes, Organic/inorganic hybrid network materials by the sol–gel approach, Chem. Mater. 8 (1996) 1667–1681.
[30] S. Pandey, S.B. Mishra, Sol–gel derived organic–inorganic hybrid materials: synthesis, characterizations and applications, J. Sol–Gel Sci. Technol. 59 (2011) 73–94.
[31] R. Ciriminna, A. Fidalgo, V. Pandarus, F. Béland, L.M. Ilharco, M. Pagliaro, The sol–gel route to advanced silica-based materials and recent applications, Chem. Rev. 113 (2013) 6592–6620.
[32] M. Catauro, F. Papale, G. Roviello, C. Ferone, F. Bollino, M. Trifuoggi, C. Aurilio, Synthesis of SiO_2 and CaO rich calcium silicate systems via sol–gel process: bioactivity, biocompatibility, and drug delivery tests, J. Biomed. Mater. Res. A 102 (2014) 3087–3092.
[33] www.mapei.it (http://www.mapei.it/public/IT/products/367_epojet_it.pdf).
[34] T.W. Swaddle, Silicate complexes of aluminium (III) in aqueous systems, Coord. Chem. Rev. 665 (2001) 219–221.
[35] W.M. Kriven, J.L. Bell, M. Gordon, Geopolymer refractories for the glass manufacturing industry, Ceram. Eng. Sci. Proc. 25 (2004) 57–79.
[36] C.F. Maitland, C.E. Buckley, B.H. O'Connor, P.D. Butlerb, R.D. Harta, Characterization of the pore structure of metakaolin-derived geopolymers by neutron scattering and electron microscopy, J. Appl. Crystallogr. 44 (2011) 697–707.
[37] E.R. Vance, J.H. Jr Hadley, F.H. Hsu, E. Drabarek, Positron annihilation lifetime spectra in a metakaolin-based geopolymer, J. Am. Ceram. Soc. 91 (2008) 664–666.
[38] J. Davidovits, Geopolymers: inorganic polymeric new materials, J. Therm. Anal. 37 (1991) 1633–1656.
[39] F. Zibouche, H. Kerdjoudj, J.B. d'Espinose de Lacaillerie, H. Van Damme, Geopolymers from Algerian metakaolin. Influence of secondary minerals, Appl. Clay Sci. 43 (2009) 453–458.
[40] C. Li, H. Sun, L. Li, The comparison between alkali-activated slag (Si + Ca) and metakaolin (Si + Al) cements, Cem. Concr. Res. 40 (2010) 1341–1349.
[41] Y.-L. Tsai, J.V. Hanna, Y.-L. Lee, M.E. Smith, J.C.C. Chan, Solid-state NMR study of geopolymer prepared by sol–gel chemistry, J. Solid State Chem. 183 (2010) 3017–3022.
[42] G. Engelhardt, D. Michael, High-resolution Solid State NMR of Silicates and Zeolites, Wiley, New York, 1987.
[43] P. Duxson, J.L. Provis, G.C. Lukey, F. Separovic, J.S.J. van Deventer, ^{29}Si NMR study of structural ordering in aluminosilicate geopolymer gels, Langmuir 21 (2005) 3028–3036.
[44] X. Yao, Z. Zhang, H. Zhu, Y. Chen, Geopolymerization process of alkali–metakaolinite characterized by isothermal calorimetry, Thermochim. Acta 493 (2009) 49–54.
[45] S.-J. Lyu, Y.-H. Hsiao, T.-T. Wang, T.-W. Cheng, T.-H. Ueng, Microstructure of geopolymer accounting for associated mechanical characteristics under various stress states, Cem. Concr. Res. 54 (2013) 199–207.
[46] D. Sakellariou, S.P. Brown, A. Lesage, S. Hediger, M. Bardet, C.A. Meriles, A. Pines, L. Emsley, High-resolution NMR correlation spectra of disordered solids, J. Am. Chem. Soc. 125 (2003) 4376–4380.
[47] P. Duxson, S.W. Mallicoat, G.C. Lukey, W.M. Kriven, J.S.J. van Deventer, The effect of alkali and Si/Al ratio on the development of mechanical properties of metakaolin-based geopolymers, Colloids Surf. A 292 (2007) 8–20.
[48] P. Duxson, J.L. Provis, G.C. Lukey, S.W. Mallicoat, W.M. Kriven, J.S.J. van Deventer, Understanding the relationship between geopolymer composition, microstructure and mechanical properties, Colloids Surf. A 269 (2005) 47–58.
[49] A. Van Riessen, W. Rickard, Geopolymers: Structure, Processing, Properties and Industrial Applications, first ed. CRC Press, 2009.
[50] M.C.M. Nasvi, P.G. Ranjith, J. Sanjayan, Effect of different mix compositions on apparent carbon dioxide (CO_2) permeability of geopolymer: suitability as well cement for CO_2 sequestration wells, Appl. Energy 114 (2014) 939–948.
[51] M.C.M. Nasvi, P.G. Ranjith, J. Sanjayan, H. Bui, Effect of temperature on permeability of geopolymer: a primary well sealant for carbon capture and storage wells, Fuel 117 (2014) 354–363.
[52] S. Hamdani, C. Longuet, D. Perrin, J.-M. Lopez-cuesta, F. Ganachaud, Flame retardancy of silicone-based materials, Polym. Degrad. Stab. 94 (2009) 465–495.